

## Characterization of Spatial Variability of Hydrogeologic Properties for Unsaturated Flow in the Fractured Rocks at Yucca Mountain, Nevada

Quanlin Zhou, Gudmundur S. Bodvarsson, Hui-Hai Liu, and Curtis M. Oldenburg

Earth Sciences Division, Lawrence Berkeley National Laboratory, Berkeley, California

### Abstract

The spatial variability of layer-scale hydrogeologic properties of the unsaturated zone (UZ) at Yucca Mountain, Nevada, is investigated using inverse modeling. The thick UZ is grouped into five hydrostratigraphic units and further into 35 hydrogeologic layers. For each layer, lateral variability is represented by the variations in calibrated values of layer-scale properties at different individual deep boreholes. In the calibration model, matrix and fracture properties are calibrated for the one-dimensional vertical column at each individual borehole using the ITOUGH2 code. The objective function is the summation of the weighted misfits between the ambient unsaturated flow (represented by measured state variables: water saturation, water potential, and pneumatic pressure) and the simulated one in the one-dimensional flow system. The objective function also includes the weighted misfits between the calibrated properties and their prior information. Layer-scale state variables and prior rock properties are obtained from their core-scale measurements. Because of limited data, the lateral variability of three most sensitive properties (matrix permeability  $k_m$ , matrix  $\alpha_m$  of the van Genuchten characterization, and fracture permeability  $k_f$ ) is calibrated, while all other properties are fixed at their calibrated layer-averaged values. Considerable lateral variability of hydrogeologic properties is obtained. For example, the lateral variability of  $k_m$  is two to three orders of magnitude and that of  $\alpha_m$  and  $k_f$  is one order of magnitude. The effect of lateral variability on site-scale flow and transport will be investigated in a future study.

### 1. Introduction

Complex geologic deposits occur at Yucca Mountain, Nevada, the potential site for a high-level nuclear waste repository. The unsaturated zone (UZ) consists of alternating sequences of variably fractured and faulted welded and nonwelded tuffs. The most important is the flow and transport in fractures and faults serving as fast paths. In the past two decades, extensive site characterization has been conducted at Yucca Mountain, including surface exploration, the drilling of a large number of deep and shallow boreholes, measurements and experimental tests, estimation of hydrogeologic properties, and flow and transport simulation, etc. [Bodvarsson, et al, 1999]. To understand the complex property distributions and their effects on flow and transport, a large number of core-scale data have been obtained. These data have been used for the analysis of hydrologic properties [Liu *et al.*, 2000], and furthermore for calibration of mean layer-scale hydrologic properties [Ahlers and Liu, 2000] for the three-dimensional mountain-scale UZ flow model. However, the lateral variability of hydrologic properties has not been investigated in the analysis and calibration of rock properties.

Lateral variability of rock properties can be seen from the variation of measured state variables and properties in the core samples at different boreholes. Flint [1998a] showed lateral variability of porosity, based on porosity measurements. Bandurraga and Bodvarsson [1999] presented a certain degree of lateral variability of matrix properties, using individual inversion based on matrix water saturation and moisture potential data. They also showed a certain degree of effect of lateral variability on radionuclide transport from the repository to water table. The reliable large variation of water saturation at different boreholes suggests that lateral variability of hydrogeologic properties may produce large variations in water saturation and (further) in percolation flux in the lateral direction. The lateral variation of fracture permeability may lead to different percolation flux patterns at different elevations. In particular, the effect of the lateral variability on the breakthrough curve of radionuclide transport at the water table and the travel time from the repository to the water table remains to be investigated.

In this study, the core-scale measured state variables of unsaturated flow were first analyzed for the ambient flow situation, and layer-scale state variables were obtained. The core-scale measured rock properties and desaturation data were then analyzed for the prior layer-scale properties. The correlation lengths of local-scale permeability were derived from its core-scale measurements. Finally, the spatial variability of three most sensitive properties (matrix permeability  $k_m$ , matrix  $\alpha_m$ , and fracture permeability  $k_f$ ) was investigated using inverse modeling.

## 2. Geologic Setting

The UZ flow model layers are classified on the basis of the geology and hydrology of the deposits at Yucca Mountain. The unsaturated zone consists of alternating sequences of variably fractured and faulted welded and nonwelded tuffs. The geologic formations have been grouped into hydrogeologic units on the basis of welding by Montazer and Wilson [1984]. The hydrogeologic units consist of the following, in order from the land surface: welded Tiva Canyon Tuff (TCw); mainly nonwelded Paintbrush Group (PTn); welded Topopah Spring Tuff (TSw); mostly nonwelded and sometimes altered Calico Hills Formation (CHn); and mostly nonwelded and altered Crater Flat undifferentiated Group (CFu). The nonwelded zones near the water table in the CHn and CFu can be subject to zeolitic alteration that reduces the matrix permeability by orders of magnitude [Bandurraga and Bodvarsson, 1999]. Furthermore, the 35 hydrogeologic layers are defined to correspond to geologic formations and/or coincident hydrogeologic unit boundaries down through the TSw. The naming convention associated with the UZ model layers and the corresponding alteration zones or geologic formations is shown in Table 3 by Liu and Ahlers [2000].

## 3. Characterization of Unsaturated Flow

The ambient unsaturated flow at Yucca Mountain is controlled by the hydrogeologic properties of rock. Information on hydrogeologic properties can be obtained from drilling (core samples in 33 boreholes), and *in situ* field characterization in the Exploratory Studies Facility (ESF) and Enhanced Characterization of Repository Block (ECRB), both of which are underground tunnels. Measurements for three different

state variables of UZ flow (water saturation, water potential and pneumatic pressure) have been obtained to improve understanding of UZ flow and estimation of hydrogeologic properties.

### 3.1. Water Saturation

A large number of water saturation measurements have been obtained at 11 deep boreholes. Water saturation data are also available in the ESF and ECRB tunnels and the north and south ramps.

Figure 1 shows the core-scale profiles of water saturation at boreholes SD-12 and UZ-16 and profiles of layer-scale water saturation. Water saturation in the TCw unit is high, while it is relatively low in the nonwelded PTn unit, where matrix intrinsic permeability is large. Within the welded TSw unit, water saturation increases with depth. In the nonwelded CHn unit and below, layer-scale water saturation distribution depends on the presence of zeolitic and vitric rocks. At borehole SD-12, the large variation in water saturation indicates the large variations in matrix permeability and capillary pressure parameters between vitric layers (of large permeability) and underlying zeolitic layers (of low permeability). The capillary pressure parameters are the inverse of characteristic capillary pressure,  $\alpha$ , and the slope parameter,  $m$ , in the van Genuchten characterization used in this study. At borehole UZ-16, no large variation in water saturation can be seen, because there are no vitric layers present between the TSw unit and zeolitic layers. The devitrified unit in CHn has water saturation much lower than that in the underlying and overlying layers. Figure 1 also shows the small variations of core-scale water saturation within each hydrogeologic layer. This variation results from the variation in local-scale matrix permeability and capillary pressure parameters.

Variation in water saturation is a “signature” of heterogeneity of matrix properties under ambient steady-state flow. Irregular variations in core-scale water saturation reflect the contrast of intrinsic permeability and capillary pressure parameters. UZ flow at Yucca Mountain is believed to be near steady state [Bodvarsson et al., 1999]. The irregular variations in water saturation may compensate for the effects of varying hydrologic properties. For example, in a low permeability layer sandwiched into upper and lower layers of higher permeability, water saturation may be higher than its neighboring layers, producing a higher relative permeability. This feature results in a small variation in the actual permeability (combination of relative permeability and intrinsic permeability of liquid phase).

### 3.2. Water Potential

Both *in situ* and core water potential measurements are available at some boreholes. Due to drying in the core-handling process, core water potential increases significantly, even for a small reduction in water saturation [Rousseau et al., 1997a, b]. For example, most core data suggest that the absolute value of the water potential at Yucca Mountain is in the range of 3-6 bars [Bodvarsson et al., 1999], while the *in situ* water potential is in range of 0.3-2.0 bars. Therefore, only *in situ* water potential is used in the inverse modeling of hydrogeologic properties for the UZ flow. *In situ* water potential data are available at boreholes NRG-6, NRG-7a, SD-7, SD-12, and UZ-7a. Less

than ten data points are available for each borehole. As a result, *in situ* water potential data play a less important role in inverse modeling than water saturation.

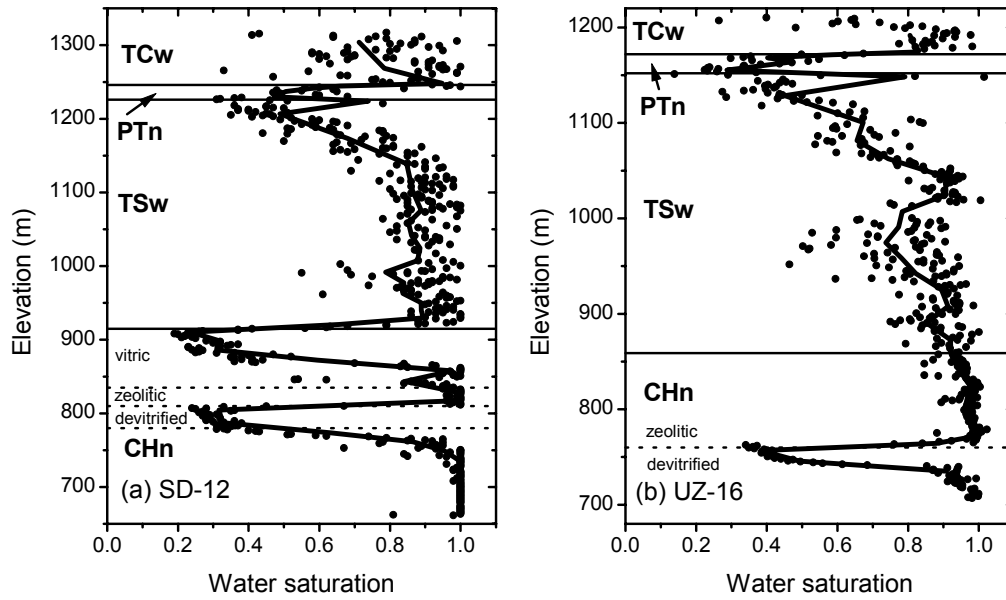


Figure 1. Vertical profiles of measured core-scale water saturation (in dots) and their layer-scale values (in solid lines) at (a) SD-12 borehole, and (b) UZ-16 borehole. The measured saturation data are from USGS [OCRWM/DOE, 1995; Rousseau et al., 1997a, b; Flint, 1998b].

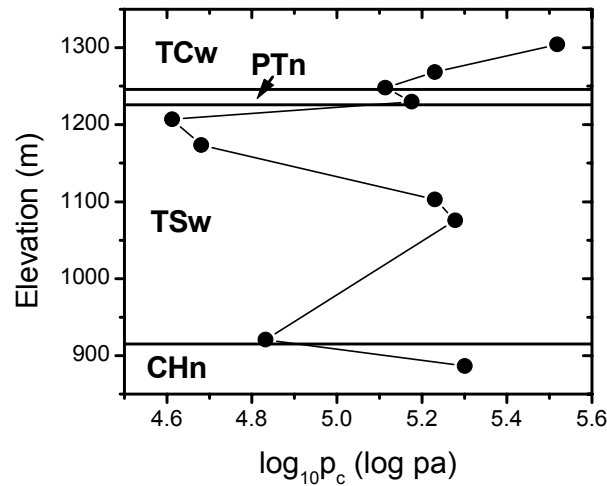


Figure 2. The vertical profile of *in situ* water potential measurements at the SD-12 borehole. Data are from USGS [OCRWM/DOE, 1995; Rousseau et al., 1997a, b; Flint, 1998b].

Figure 2 shows the measured profile of the *in situ* water potential at borehole SD-12. Variation in water potential ( $p_c$ ) is small in comparison with that of water saturation. This is because at a low permeability layer, the characteristic capillary pressure ( $\alpha^{-1}$ )

may be high, while high water saturation produces a low normalized capillary pressure ( $p_c \alpha$ ). Both effects compensate for one another and thereby maintain a water potential field of small variation. The small ambient variation of water potential shows that the capillary pressure gradient is much smaller than the gravity gradient, resulting in a gravity-driven liquid flow at Yucca Mountain. For example, the maximum capillary pressure gradient is 17% of the gravity pressure gradient.

### 3.3. Pneumatic Pressure

Both water saturation and potential measurements can be employed to calibrate matrix properties, because both state variables are directly related to matrix properties. Pneumatic pressure measurements are very useful in estimating fracture permeability, which is the key parameter in the welded geologic units, where fracture flow is dominant.

Pneumatic pressure is indicative of naturally occurring subsurface gas flow caused by barometric pressure changes. Some boreholes were instrumented with isolated pressure transducers or pressure monitoring ports. These kinds of data are available at boreholes SD-7, SD-12, NRG-6, NRG-7a, and UZ-7a. The pneumatic records at all boreholes show common characteristics [Ahlers et al., 1999]. Sensors in the TCw record small to zero amplitude attenuation or phase lag with respect to the surface barometric signal. Sensors in the PTn unit record increasing attenuation and lag with depth below the top of the PTn. In most boreholes, sensors in the TSw record the same amount of attenuation and lag over the entire vertical interval of the TSw. Horizontally within the TSw, the observed attenuation and lag vary and appear to be governed by the thickness of the overlying PTn. It can be seen that significant attenuation occurs within the PTn unit, where there are fewer fractures.

## 4. Local-Scale Hydrogeologic Properties

Direct measurement of hydrogeologic properties has been conducted at different boreholes for porosity, intrinsic permeability, and capillary pressure parameters. The data are representative of small-scale properties at core scale. The core size, in general, is of 0.07 m diameter and 2-3 m in length. The local-scale measurements of intrinsic permeability and capillary pressure parameters can be used to calculate their prior layer-scale values for the following calibration model.

### 4.1. Intrinsic Permeability

Measurements of intrinsic permeability are obtained at seven deep boreholes (SD-6, SD-7, SD-9, SD-12, UZ-14, UZ-16, and WT-24). For each of the boreholes, measurements are not available at all hydrogeologic layers. Figure 3 shows the vertical profile of measured intrinsic permeability at borehole UZ-16. Matrix permeability in the TCw unit is relatively small, but it is large in the thin PTn unit. The permeability in the entire TSw unit is also relatively small, with a large variability (five orders of magnitude). In addition, matrix permeability is too low to be measured for a number of core samples, a condition we refer to as “nondetected”. Matrix permeability is low with small variability in the zeolitic layers, while in the devitrified layers, the measured permeability is relatively high.

The solid line in Figure 3 shows the geometric mean of measured permeability within each UZ model layer in the conceptual model. When both nondetected and detected data are available at a layer, the geometric mean was obtained based on the assumption of log-normal distribution of permeability, with the nondetected data points ranked at the end of lowest permeability.

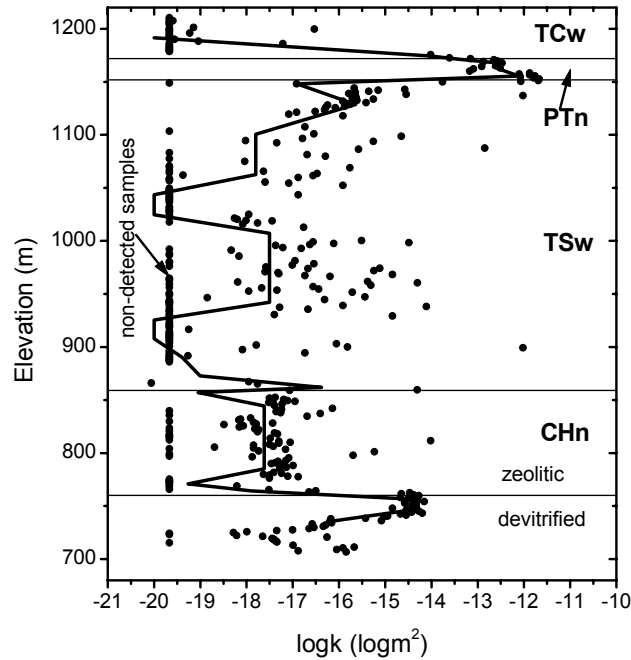


Figure 3. The vertical profile of measured core-scale intrinsic permeability (in dots) and layer-scale permeability (in solid line) at borehole UZ-16. Data are from USGS [OCRWM/DOE, 1995; Rousseau et al., 1997a, b; Flint, 1998b].

## 4.2. Capillary Pressure Parameters

Capillary pressure parameters ( $\alpha$  and  $m$  for the van Genuchten characterization) were estimated from the desaturation curve data. The desaturation experiments were conducted for 75 core samples obtained from three boreholes (SD-9, UZ-16 and UZN-27). At each hydrogeologic layer, there is at least one set of data for the water saturation and capillary pressure curve.

## 4.3. Fracture Permeability

Fracture permeability was calculated for the UZ model layers based on air permeability inferred from air-injection tests conducted in vertical boreholes and ESF alcoves and niches [Rousseau et al., 1997a, b; Liu et al., 2000]. The geometric mean of the fracture permeability is assumed to reflect upscaling of this property from local-scale to layer-scale. The resulting fracture permeability in each layer is used as prior information in the following calibration model.

#### 4.4. Correlation Lengths

At Yucca Mountain, core-property measurements were not designed to obtain accurate spatial correlation lengths because the spacing of measurements is not uniform in the vertical direction. In the horizontal direction, only some shallow boreholes with porosity measurements are located within a correlation length, and all deep boreholes with permeability measurements are located farther apart than a correlation length. Therefore, correlation lengths of matrix permeability at the local scale are roughly estimated from available core-scale measurements.

The vertical correlation length is estimated from permeability data in deep boreholes. The sample spacing of some 2-5 m within some layers at a borehole does not vary significantly, making it possible to calculate the correlation lengths for such layers. Such quality permeability data are available only for several layers at borehole UZ-16 and two other deep boreholes. For each of such layers, we estimated the vertical correlation length using the permeability data with quasi-uniform spacing. The exponential covariance model is used. The estimated vertical correlation length ( $\lambda_z$ ) at different layers varies from 5 to 20 m, with an average of 10 m. Figure 4a shows the estimated vertical correlation length in layer TSw34 at borehole UZ-16.

The horizontal correlation length is estimated from porosity measurements available in layers within several clusters of shallow boreholes. For example, boreholes UZN-53 through UZN-55 are less than 100 m apart (Flint, 1998a). For two close boreholes, the covariance function, normalized by standard deviations, is estimated for a layer with a number of data points ( $\geq 10$ ) in both boreholes. The average covariance function is then calculated for all available layers, leading to a data point in fitting the horizontal correlation length. Figure 4b shows the average horizontal correlation length ( $\lambda_{xy}$ ) of approximately 120 m, estimated from porosity data in shallow boreholes. It is assumed that this horizontal correlation length can be used to approximate that of local-scale permeability, because the correlation between porosity and permeability obtained from their measurement is good (Flint, 1998a).

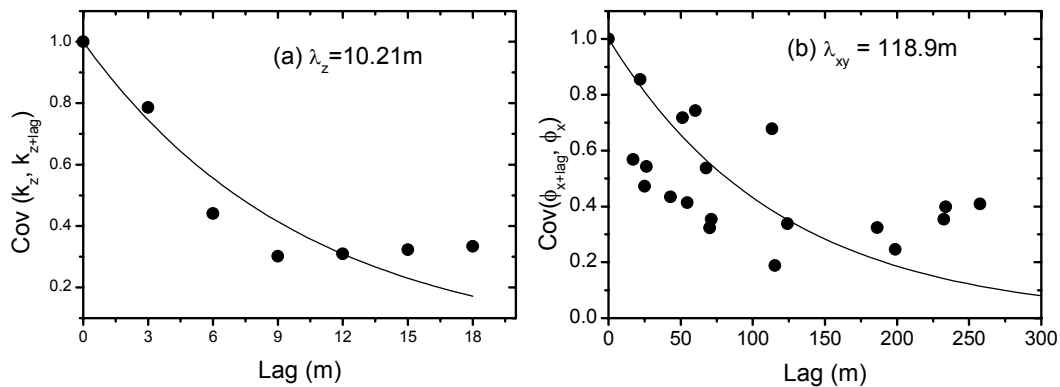


Figure 4. Estimation of correlation lengths in (a) the vertical and (b) horizontal directions.

## 5. Characterization of Layer-Scale Rock Properties

Hydrogeologic properties in different units and layers vary significantly in the vertical direction due to different geologic processes and rock alteration. The layer-scale properties reflect bulk effects within each layer in the calibration model to be consistent with the current three-dimensional UZ flow model. In each layer, the lateral variability of layer-scale hydrogeologic properties is represented by the variations in their calibrated values at different boreholes.

Two calibration steps are used to reduce the uncertainty in the estimated rock properties. In the first step, mean values of seven sets of layer-scale properties (matrix permeability  $k_m$ , matrix  $\alpha_m$ , matrix  $m_m$ , fracture permeability  $k_f$ , fracture  $\alpha_f$ , fracture  $m_f$ , and fraction of active fractures  $\gamma_f$ ) are calibrated using simultaneous inverse modeling (SIM) [Ahlers and Liu, 2000]. For each layer, only one value for each set of hydrogeologic properties needs to calibrate. Data at different boreholes are considered as different samples and only one calibration process is conducted for all boreholes. In the second step, the lateral variability of three most sensitive sets of properties ( $k_m$ ,  $\alpha_m$ , and  $k_f$ ) is further calibrated. At a borehole, one parameter needs to be estimated for each set of properties within a layer if the layer exists with sufficient measurement data. All other sets of properties are fixed at their values obtained by SIM in the first step. In this step, a calibration process is conducted independently for each deep borehole. In what follows, only the second step is presented.

In a calibration process, calibration of matrix properties and fracture permeability is done iteratively. First, matrix properties are calibrated using water saturation and potential data through steady-state single-phase flow simulation. Second, fracture permeability is calibrated using pneumatic pressure data through transient simulation of gas and water flow, and all matrix properties are fixed at their newly calibrated values. The iterative process continues until convergence is obtained.

For a deep borehole of interest, the flow system is a vertical column from the top surface to the water table. It is assumed that the flow of gas or/and liquid is one-dimensional within the column. For the forward simulation of single-phase flow (liquid flow), the infiltration rate is specified on the top boundary and a water saturation of 1.0 is specified on the bottom water table. For the forward simulation of water-gas flow, the surface barometric pressure with transient change and the infiltration rate of water are specified at the top boundary, while no-flow condition is assumed at the bottom of the vertical column for both gas and water phases. This assumption is based on travel times for change in barometric pressure and infiltration from the land surface to the bottom being much longer than the total simulation time of the transient process. The TOUGH2 code is used for the forward simulation of single-phase liquid flow and two-phase flow (gas-water flow) [Pruess et al., 1999]. The ITOUGH2 code is used for parameter estimation [Finsterle, 1999].



## 5.1. Matrix Properties

In a calibration process for a deep borehole, matrix properties are calibrated within the framework of steady-state unsaturated liquid flow. Their prior information was obtained from measured intrinsic permeability and capillary pressure parameter  $\alpha_m$  values. The same prior information and initial guess (the SIM calibrated results) of  $\alpha_m$  are used for all boreholes, because there are not enough desaturation data. When permeability measurements are available within a layer, their geometric mean is used as prior information; otherwise, the SIM calibrated value is used. The objective function consists of mismatch of water saturation, water potential, and the mismatch of the resulting properties and their values of prior information. Different kinds of mismatches and those at different layers are weighted based on their standard deviation.

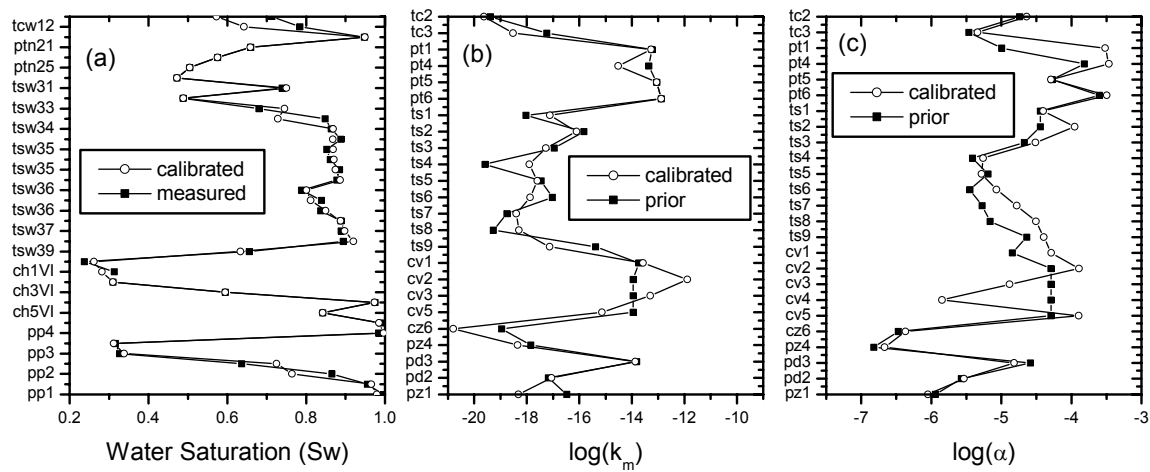


Figure 5. Match of (a) the measured water saturation profile and simulated one at the calibrated properties for borehole SD-12, (b) the prior information and the calibrated values of matrix permeability, and (c) the prior information and calibrated values of matrix  $\alpha$ . The measured water saturation data are from USGS [OCRWM/DOE, 1995; Rousseau et al., 1997a, b; Flint, 1998b].

Figure 5 shows matches between water saturation measurements and the simulated value at the final calibrated properties for borehole SD-12, as well as the mismatch of matrix permeability and  $\alpha$  between their prior information and calibrated values. It can be seen that the match for calibrated and measured water saturation is good. The difference between calibrated properties and their prior information reduces the objective function by some two orders of magnitude for SD-12 and other boreholes. Note that in the simultaneous inverse modeling, the matrix and fracture properties at ch1v through ch5v layers are assumed to be identical. In the current individual inverse modeling, properties at these layers are allowed to vary. This same treatment is applied for ch2z through ch5z layers. In this way, the match of state variables in these layers is improved because the properties in these layers are very sensitive.

## 5.2. Fracture Properties

Fracture permeability is calibrated in the framework of transient gas-water flow, using the pneumatic pressure data, after the matrix properties are determined. These data were collected from sensors at different elevations in some deep boreholes (NRG-6, NRG-7a, SD-7, and SD-12). There are just four sensors in each of the above boreholes. The pneumatic pressure measured at a sensor reflects the cumulative effects of permeability in all layers above the sensor. To improve the reliability of the calibrated fracture permeability, a factor (ratio of calibrated value to the prior information) common for the entire PTn or TSw is used. The permeability in each TCw layer is directly calibrated. Fracture permeability at each layer below TSw unit is fixed at its SIM calibrated value, because there are too few data available to independently determine these during the calibration process. The match of measured and calibrated pneumatic pressure at all sensors is very good for all four boreholes (not shown).

## 5.3. Lateral Variability of Properties

The lateral variability of the three selected layer-scale properties:  $k_m$ ,  $\alpha_m$ , and  $k_f$  is represented by the difference of their calibrated values at different boreholes. We use a random variable representing a set of properties within a layer, and obtain the mean and standard deviation of the random variable. We obtain a calibrated value (a sample) for this property at an individual borehole. The number of samples depends on the number of boreholes used in the calibration processes and the presence of the layer. Because all deep boreholes available for the calibration are located much farther apart than the horizontal correlation length, samples can be treated as independent. The mean and standard deviation of each random variable at each layer are calculated.

Figure 6 shows the lateral variability of  $k_m$  and  $\alpha_m$  at different hydrogeologic layers. The solid line represents the vertical profile of mean value of these properties, while the dotted line represents the SIM result. The scatter points represent calibrated values at different boreholes obtained by individual inverse modeling. The lateral variability of  $k_m$  is two to three orders of magnitude. Most importantly, the lateral variability is smaller than the dominant vertical variability of permeability at different geologic units. For example, the variation of the mean permeability between the TSw and CHn units is five to six orders of magnitude; mean permeability in the TSw and PTn varies by five orders of magnitude. The matrix  $\alpha_m$  varies much less than  $k_m$ . Lateral variability of  $\alpha_m$  in general is one order of magnitude. The vertical profile of the mean  $\alpha_m$  is very similar to that obtained by simultaneous inverse modeling.

Figure 7 shows the lateral variability of layer-scale  $k_f$ , as well as mean  $k_f$  value (solid line) and the SIM calibrated result (dotted line) [Ahlers and Liu, 2000]. The mean  $k_f$  in the PTn unit is very close to its corresponding SIM calibrated result. In the TSw unit, the mean  $k_f$  is smaller than the SIM result by half an order of magnitude. This is because in the SIM calibration, much attention was paid on the match between calibrated and measured pneumatic pressure at borehole SD-12.

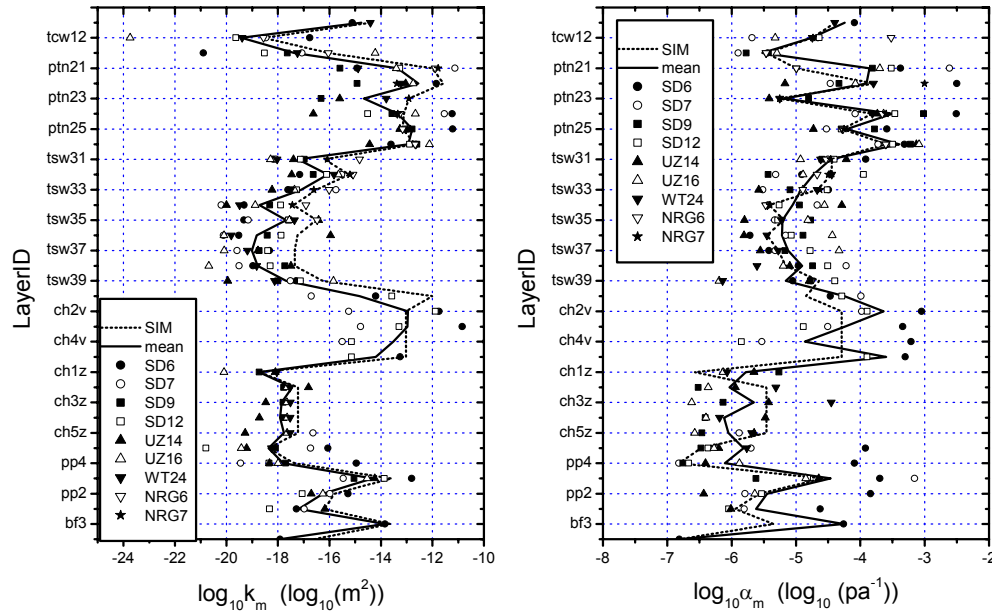


Figure 6. Spatial variability of matrix permeability and  $\alpha$  at different hydrogeologic layers obtained by individual inverse modeling using borehole measurements.

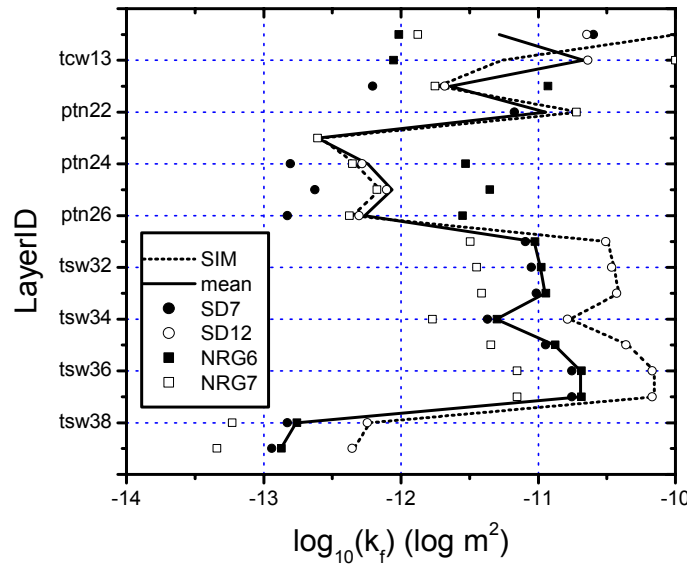


Figure 7. Spatial variability of fracture permeability at different hydrogeologic layers at four boreholes with available measurements

## 6. Conclusion

In the conceptual model currently used for the site characterization of Yucca Mountain, the lateral variability of hydrogeologic properties and its effect on flow and transport is neglected by assuming uniform layer-scale properties at each hydrogeologic

layer. In this research, the lateral variability of the three most sensitive hydrologic properties (matrix permeability  $k_m$ , and matrix  $\alpha_m$ , and fracture permeability  $k_f$ ) was investigated using individual inverse modeling. The calibration of the three properties at each deep borehole was performed using measurements of water saturation, water potential and pneumatic pressure, and those of intrinsic permeability and desaturation curve data. All other hydrologic properties are fixed at their optimal laterally averaged values obtained by simultaneous inverse modeling. Significant lateral variability of the three properties was obtained. For example, matrix permeability varies over two to three orders of magnitude for a layer. The lateral variability of matrix permeability is smaller than the dominant vertical variability of five to six orders that occurs between hydrostratigraphic units. The mean value of layer-scale properties is different from the laterally layer-averaged values obtained by simultaneous inverse modeling.

## Acknowledgments

Thanks are due to S. Finsterle and C. F. Ahlers for their help in this work. This work was in part supported by the Director, Office of Civilian Radioactive Waste Management, U.S. Department of Energy, through Memorandum Purchase Order EA9013MC5X between Bechtel SAIC Company, LLC and the Ernest Orlando Lawrence Berkeley National Laboratory (Berkeley Lab).

## References

- Ahlers, C.F. and Liu, H.H., 2000. *Calibrated Properties Model*. Report MDL-NBS-HS-000003. Berkeley, California: Lawrence Berkeley Laboratory. Las Vegas, Nevada: CRWMS M&O.
- Ahlers, C. F., S. Finsterle, and G. S. Bodvarsson, 1999. Characterization and prediction of subsurface pneumatic response at Yucca Mountain, Nevada. *Journal of Contaminant Hydrology*, 38 (1-3), 47-68.
- Bandurraga, T. M., and G. S. Bodvarsson, 1999. Calibrating hydrogeologic parameters for the 3-D site-scale unsaturated zone model of Yucca Mountain, Nevada, *Journal of Contaminant Hydrology*, 38 (1-3), 25-46.
- Bodvarsson, G. S., W. Boyle, R. Patterson, and D. Williams, 1999. Overview of scientific investigations at Yucca Mountain- the potential repository for high-level nuclear waste, *Journal of Contaminant Hydrology*, 38 (1-3), 3-24.
- Findterle, S., 1999. *ITOUGH2 User's Guide*, Report LBNL-40040, UC-400, Berkeley, California: Lawrence Berkeley National Laboratory.
- Flint, L. E., 1998a. *Characterization of hydrogeologic units using matrix properties*, Yucca Mountain, Nevada, USGS Water resources investigation report 97-4243, Denver, Colorado.
- Flint, L. E., 1998b. Matrix properties of hydrogeologic units at Yucca Mountain, Nevada, U.S. Geological Survey Open-File Report, MOL. 19970324.0046, GS950308312231.002 (Q). U.S. Geological Survey, Denver, CO.
- Liu, H.H., Ahlers, C.F. and Cushey, M.A., 2000. *Analysis of Hydrologic Properties*. Report ANL-NBS-HS-000002. Berkeley, California: Lawrence Berkeley Laboratory. Las Vegas, Nevada: CRWMS M&O.

- Liu, H.H., Doughty, C., and Bodvarsson, G.S., 1998. An active fracture model for unsaturated flow and transport in fractured rocks, *Water Resources Research*, 34, 2633–2646.
- Montazer, P. and Wilson, W.E., 1984. *Conceptual Hydrologic Model of Flow in the Unsaturated Zone, Yucca Mountain, Nevada*. Water-Resources Investigations Report 84-4345. Lakewood, Colorado: U.S. Geological Survey.
- OCRWM, DOE, 1995. Technical Data Catalog. Yucca Mountain Site Characterization Project.
- Pruess, K., C. Oldenburg, and G. Moridis, 1999. *TOUGH2 user's guide*, Report LBNL-43134, Berkeley, California: Lawrence Berkeley National Laboratory.
- Rousseau, J.P., Loskot, C.L., Thamir, F., and Lu, N., 1997a. *Results of borehole monitoring in the unsaturated zone within the main drift area of the Exploratory studies facility*, Yucca Mountain, Nevada, USGS Milestone Report SPH22M3, Denver, Colorado.
- Rousseau, J.E., Kwicklis, E.M. Grillies D.C., 1997b. *Hydrogeology of the unsaturated zone, north ramp area of the exploratory studies facility*, Yucca Mountain, Nevada. US Geological Survey Water Resources Investigation Report 98-4045, Denver, Colorado.